Lifshitz and Excited State Quantum Phase Transitions in Microwave Dirac Billiards

B. Dietz, M. Miski-Oglu, N. Pietralla, A. Richter, L. von Smekal, and J. Wambach
Institut für Kernphysik, Technische Universität Darmstadt, 64289 Darmstadt, Germany

F. Iachello
Center for Theoretical Physics, Sloane Physics Laboratory, Yale University, New Haven, CT 06520-8120, USA

(Dated: April 18, 2013)

We present experimental results for the density of states (DOS) of a superconducting microwave Dirac billiard. Such systems serve as models for the electronic properties of finite graphene sheets. The DOS exhibits two sharp peaks which evolve into van Hove singularities with increasing system size. These divide the Fermi surface into regions governed by the relativistic Dirac equation and by the non-relativistic Schrödinger equation, respectively. We demonstrate that there a topological transition appears as a neck-disrupting Lifshitz transition in the number susceptibility and as an excited state transition in the electronic excitations. Furthermore, we recover the finite-size scaling typical for excited state quantum phase transitions involving logarithmic divergences.

PACS numbers: 05.70.Fh,42.70Qs,71.20.-b,73.22.Pr

Introduction.– Graphene, a monolayer of carbon atoms forming a hexagonal lattice, has attracted a lot of attention in recent years due to its extraordinary properties associated with the shapes of the conduction and the valence band. These touch each other conically, thus implying a linear dispersion relation. As a consequence, close to these so-called Dirac points excitations are decribed by a Dirac Hamiltonian [1]. The inset of Fig. 1

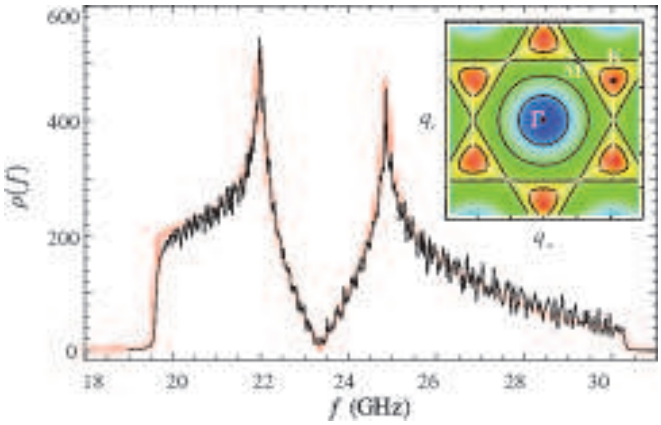

FIG. 1: (Color on line) Density of states $\rho(f)$ obtained from the resonance spectrum (see text below) of a microwave Dirac billiard (black line). The red line results from a tight-binding model [2]. The region of low density around the Dirac frequency $f_D = 23.36$ GHz is delimitated by two sharp peaks, van Hove singularities, at $f_{vH}^- = 21.98$ GHz and $f_{vH}^+ = 24.87$ GHz. The inset shows isofrequency lines of the numerically determined Fermi surface of propagating modes in the quasi-momentum plane (q_x, q_y) (see text).

shows isofrequency lines [3] of the band structure (black lines), i.e., the Fermi surface in the plane of the quasi-momentum vector components (q_x, q_y). The Dirac (K) points are located at the corners of the Brillouin zone (BZ). In their vicinity the isofrequency lines form circles, that deform into triangles with the distance from them. This *relativistic* regime is bordered by saddle points at the M points. At the centre of the Brillouin zone, the Γ point, the conduction (valence) band has a maximum (minimum). In its vicinity the isofrequency lines form circles and the Fermi surface has a parabolic shape. There the non-relativistic Schrödinger equation applies. Accordingly, the Fermi surface can be separated into two independent *relativistic* regions and one *non-relativistic* one. The change of the topology takes place at the M points, where the Dirac cones merge into the parabolically shaped surface. At the energies of the M points the density of states ρ (DOS) diverges logarithmically in an infinitely extended graphene sheet [4]. These are the so-called van Hove singularities, which were predicted to exist in general in 2-dimensional crystals with a periodic structure [5].

The topological phase transition associated with these singularities may be realized either by changing the lattice structure [6, 7] or by applying a chemical potential, see Ref. [8]. We will demonstrate in this letter that it can be identified with a neck-disrupting ground-state Lifshitz transition [9]. Furthermore we will show that it can also be interpreted as an excited state quantum phase transition (ESQPT) in the single-particle excitations. Transitions of the latter type have been observed in the equivalent bosonic system. A particularly close analogy with the present case is provided by the 2-dimensional vibron model [10] describing transverse vibrations of molecules, but ESQPTs have been studied in many other models as well [11–14], including a detailed study of quasi-spin systems [15]. We investigated properties of the DOS of graphene experimentally in its microwave analog and recovered this finite-scaling behavior, thus corroborating its universal nature. Figure 1 presents the density of states (DOS) of the microwave Dirac billiard. Its experimental determination is described in the next section.

Experiment.– Microwave billiards have been used since two decades as analog systems for the study of non-relativistic quantum phenomena [16, 17]. The present

letter is about experiments which were performed with microwave photonic crystals. Generally, photonic crystals [18, 19] are the optical analog of a solid and the frequencies of wave propagation as function of the two components of the quasi momentum exhibit a band structure. The microwave photonic crystals were composed of metallic cylinders constituting a triangular lattice [20, 21] and squeezed between two metal plates. The structure of the crystal's first two bands is similar to the Fermi surface of graphene, that is, it is Dirac like in the vicinity of their touch points [22]. There, the scalar Helmholtz equation describing the sytem reduces to the Dirac equation of massless spin-1/2 particles. The linear dispersion relation in graphene is due to the presence of two interpenetrating triangular lattices with threefold rotational symmetry in the hexagonal lattice [23]. In the triangular photonic crystal the honeycomb lattice is formed by the voids enclosed by, respectively, three cylinders. We use this analogy to experimentally investigate relativistic phenomena occurring in graphene. Various effects have already been studied as, e.g., pseudo-diffusive transport near the Dirac point [24–26], the quantum Hall effect [27], Zitterbewegung [24], and edge states [25, 26, 28].

Here we present results associated with the properties of the DOS determined experimentally for two superconducting Dirac billiards [26]. They were constructed by enclosing a photonic crystal in a rectangular microwave billiard. The rectangular billiard basins containing the metallic cylinders were milled out of a brass plate with side lengths 420.0×249.4 mm^2. One Dirac billiard contained 267 metallic cylinders and had the lattice constant $a_L = 20$mm, the other one 888 with $a_L = 12$mm. The radius of the cylinders was $R = a_L/4$. Figure 2 displays a photograph of the Dirac billiard with 888 cylinders. The brass lids and the basin were lead coated to

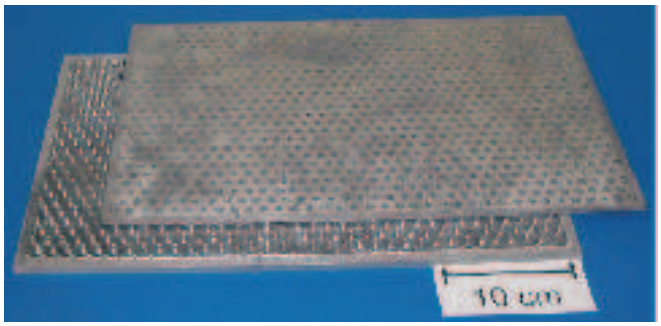

FIG. 2: (Color on line) Photograph of the superconducting microwave Dirac billiard containing 888 metal cylinders. It is constructed from brass and coated with lead. The lid is shifted with respect to the billiard body.

achieve superconductivity at liquid helium temperature. To ensure a good electrical contact the lids were screwed tightly to each cylinder. The height of the Dirac billiards was $h = 3$mm. Hence, up to the maximum frequency of 50 GHz, only the lowest transverse magnetic mode with the electric field vector perpendicular to the top

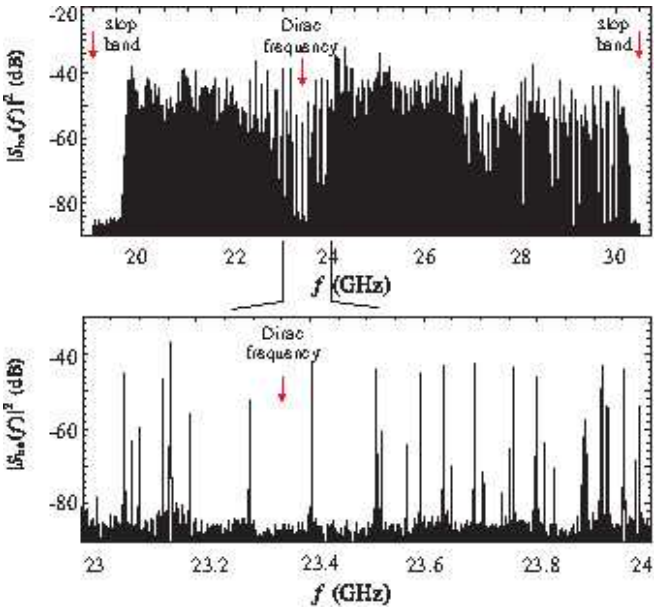

FIG. 3: A measured transmission spectrum of the microwave Dirac billiard depicted in Fig. 2 (upper panel). It is terminated by two stop bands, where no wave propagation is possible. The lower panel shows a zoom into the region of particularly low resonance density around the Dirac frequency.

and bottom plates was excited. Accordingly, the vectorial Helmholtz equation reduces to a scalar one which is mathematically identical to the Schrödinger equation of the corresponding 2-dimensional multiple-scattering problem.

Microwave power was coupled into and out of the resonator via wire antennas, that reached a few millimeters into the resonator through holes in the lid, for the measurement of the resonance spectra. A Vector Network Analyzer (VNA) measured the relative phase and amplitude of the output to the input signal. In the upper panel of Fig. 3 a transmission spectrum of the Dirac billiard with 888 cylinders measured in the frequency region between 19.5 GHz and 30.5 GHz is depicted. It is bordered by two stop bands corresponding to the band gaps in the band structure where no wave propagation is possible. Furthermore, we observe a region with an exceptionally low resonance density around the Dirac frequency of the Dirac points. The lower panel of Fig. 3 shows a zoom into that region. Transmission spectra were measured with all possible combinations of two out of a total of five antennas attached to the lid at different positions. Since the resonances had high-quality factors $Q > 5 \cdot 10^5$, we could resolve all resonances and determined 1651 eigenfrequencies.

Figure 1 shows the DOS $\rho(f)$ obtained from the measured resonance spectra, i.e., the number of states per frequency interval versus the frequency of the centre of the interval. We chose a frequency interval of 100 MHz. The red curve was computed based on a tight-binding approach [2] which takes into account not only the nearest-

neighbor, but in addition the second-nearest neighbor coupling and also the overlap integral between the wave functions located at neighboring voids [26]. In the region of low density the DOS vanishes linearly around the Dirac frequency $f_D = 23.36$ GHz with $|f - f_D| \to 0$. It corresponds to the *relativistic* region in the Fermi surface of graphene, i.e., the propagation of electromagnetic waves is governed by the Dirac equation [22]. This region is delimitated by two sharp peaks at $f_{vH}^- = 21.98$ GHz and $f_{vH}^+ = 24.87$ GHz, the van Hove singularities [5]. In the frequency range below f_{vH}^- and above f_{vH}^+ the Helmholtz equation reduces to the Schrödinger equation of the corresponding quantum billiard [16, 17]. This defines the *non-relativistic* region. A closer look at the experimental DOS reveals, that the amplitudes and the typical frequencies of the oscillations of the experimental DOS are smaller in the frequency range between the two van Hove singularities than below and above. This already indicates that both regions are governed by different wave equations.

At the van Hove singularities the DOS diverges logarithmically. This happens strictly only in an infinitely extended graphene sheet or photonic crystal. In the Dirac billiards used in the experiments, however, the sharp peaks at $f_{\rm vH}^{\pm}$ have a finite height $\rho^{\max}$. We determined it for the experimental DOS of the two microwave Dirac billiards, and also performed numerical studies with photonic crystals of various sizes and shapes. For a comparison of these results we rescaled the frequencies such that the distance $f_{vH}^+ - f_{vH}^-$ between the van Hove singularities, i.e., the group velocity, was the same for all systems. We chose the rescaling $f \to \tilde{f}$ such that $\tilde{f}_{vH}^+ - \tilde{f}_{vH}^- = 2$. The experimental and numerical studies revealed that the maxima of the DOS, $\rho^{\max}$, or rather those of the renormalized DOS, $n^{\max} = \frac{f_{\rm vH}^+ - f_{\rm vH}^-}{2}\rho^{\max}$, behave like

$$n^{\max} \simeq aN_c\,(\ln(N_c) + b) \tag{1}$$

with N_c the number of unit cells, i.e., of hexagons formed by the voids in the photonic crystal. The quantities a and b are fit parameters, where the latter depends on the geometry of the billiard, i.e., is system dependent, while the former takes a similar value $a \sim 0.145 - 0.155$ for all cases, i.e., seems to be universal. This finite-size scaling, typical of an ESQPT [15], and the fate of the isofrequency lines at the saddle points (see inset in Fig. 1) suggests a description in terms of a neck-disrupting Lifshitz transition [9]. We note, however, that all properties of the DOS that we observe in photonic crystals can also be obtained from the DOS for the vibrations perpendicular to the plane of an hexagonal lattice, as shown by Hobson and Nierenberg [29] in 1953. Except for the choice of the frequency scale their result coincides with the analytical expression for the DOS [4] investigated in the following two sections.

Neck-disrupting Lifshitz transition in graphene.– In order to illustrate the relation between the van Hove singularity in the DOS and the neck-disrupting Lifshitz transition in the analogous fermionic band structure of graphene, we computed the number susceptibility from the particle-hole polarization function, the Lindhard function [30]. For this we used the simplest tight-binding model, which takes into account only nearest-neighbor hopping of strength t [2, 4]. Many aspects concerning the electronic excitations in graphene at weak coupling [4] can be studied analytically with this model to exemplify more general effects [32]. The retarded polarization function $\Pi^R(\omega, \vec{p}; \mu)$, with ω the excitation frequency, $\vec{p}$ the vector of momentum transfer and μ the chemical potential [33, 34], is a sum of particle-hole transitions within the same band, Π_+^R, i.e., *intraband* transitions and those arising from *interband* transitions between the two bands, Π_-^R. The polarization function yields for the (zero-temperature) number susceptibility [33]

$$\chi = \lim_{\vec{p}\to 0}\lim_{\omega\to 0}\Pi^R(\omega, \vec{p}; \mu) = \frac{\rho(\mu)}{A}. \tag{2}$$

Hence, it coincides with the DOS $\rho(\omega)$ per area A of the graphene sheet at the Fermi surface $\omega = \mu$. It should be noted that only intraband transitions contribute.

In Ref. [4] the zero of the DOS, identified with the Dirac point, is located at $\mu = 0$, the van Hove singularities are at $\mu = \pm t$ and the band gaps start at $\mu = \pm 3t$. When the chemical potential is chosen near one of the van Hove singularities we readily obtain from the analytical expression Eq. (14) in Ref. [4]

$$\chi \simeq \frac{3N_c}{2\pi^2 At}\Big(-\ln|z| + 2\ln 2 + \mathcal{O}(z)\Big)\,, \tag{3}$$

where we introduced the parameter $z = (|\mu| - t)/t$. Note the logarithmic divergence for $z \to 0$, which may be related to the neck-disrupting Lifshitz transition in two dimensions [9, 35].

As in Dirac billiards, the susceptibility or DOS does not diverge in a graphene sheet of finite area. To see how the heights of its maxima scale with the area we used periodic boundary conditions and integrated Eq. (3) over a small interval $\Delta z = (2\pi)^2/N_c$ around the singularity. We again rescaled the energies such that the distance between the maxima equals two. Then we obtain for the height of the maxima of the renormalized DOS

$$n^{\max} = t\rho^{\max} \simeq \frac{3}{2\pi^2}\,N_c\,\Big(\ln N_c - 2\ln\pi + 1 + \mathcal{O}(1/N_c)\Big)\,. \tag{4}$$

Note that $\frac{3}{2\pi^2} \simeq 0.15$, thus confirming the experimental and the numerical findings, c.f., Eq. (1). Thus the height of the maxima of the susceptibility at the van Hove singularities scales as $t\chi^{\max} = n^{\max}/A \sim \ln N_c$, in accordance with the finite-size scaling of a neck-disrupting Lifshitz transition.

The divergence of χ as $z \to 0$ is caused by the infinite degeneracy of ground states of the 2-dimensional system when the Fermi surface passes through a van Hove singularity. In the thermodynamic sense this can be considered as a zero-temperature quantum phase transition

with control parameter $|\mu|$. However, unlike the cases of first- or second-order phase transitions, the susceptibility does not diverge with a power law in z but logarithmically. Furthermore, the transition is due to a change of topology of the Fermi surface with no order parameter in the strict sense.

Excited state quantum phase transition in the electronic excitations.– In the following we will present a quasi-order parameter and demonstrate that, as in the equivalent bosonic system [10–15], the singularity of the single-particle DOS as function of the excitation frequency can also be interpreted as an ESQPT in the spectrum of particle-hole excitations. For this we analyzed the polarization function at zero-momentum transfer, $\Pi^R(\omega, \vec{p}=0; \mu)$. The associated spectral distribution $\rho_{\rm ph}(\omega)$ is given by [36]

$$\rho_{\rm ph}(\omega) = Z_{-1} \lim_{\vec{p}^2 \to 0} \frac{\omega}{2\pi \vec{p}^2} \, {\rm Im}\, \Pi^R(\omega, \vec{p}; \mu) \; , \qquad (5)$$

with the normalization

$$Z = \lim_{\vec{p}^2 \to 0} \int_0^\infty d\omega \frac{\omega}{2\pi \vec{p}^2} \, {\rm Im}\, \Pi^R(\omega, \vec{p}; \mu) \; . \qquad (6)$$

It can be separated into contributions Z_+ from intraband, respectively, Z_- from interband transitions. Here, Z_+ is related to the f-sum rule [34, 37, 38], which expresses the conservation of the number of particles in terms of an identity. Indeed, Z_+ is fixed due to charge conservation via this rule in terms of the 2-dimensional charge carrier density n_c and mass m, $Z_+ = \frac{n_c}{4m}$. Near the centre of the Brillouin zone we have $n_c = p_F^2/(4\pi)$ and $m = \sqrt{3} N_c/(tA)$ and the contribution from interband transitions behaves as $Z_-(\mu) \simeq \frac{1}{108} \frac{1}{8\pi} (3t - |\mu|)^3$. Hence it is suppressed such that $Z(\mu) \approx Z_+(\mu)$, and the sum rule is readily verified,

$$Z(\mu) \simeq \frac{1}{8\pi} \, (3t - |\mu|) = \frac{1}{8\pi} \, \frac{p_F^2}{2m} = \frac{n_c}{4m} \, . \qquad (7)$$

This approximation holds as long as one restricts to intraband transitions and to the non-relativistic Fermi liquid regime either below or above the two van Hove singularities, i.e., for $|\mu| > t$. Near the Dirac cone, where $|\mu| \ll t$, on the other hand, the intraband transitions yield

$$Z_+(\mu) \simeq \frac{|\mu|}{8\pi} = \sqrt{\frac{n_c'}{2\pi}} \, \frac{v_F}{4} \, , \qquad (8)$$

with $n_c' = \mu^2/(2\pi v_F^2)$. Thus, there the intraband f-sum rule scales with the square root of the carrier density n_c' relative to half filling. However, the contribution of the interband transitions to Z,

$$Z_-(\mu) \simeq \frac{\pi t}{24\sqrt{3}} - \frac{|\mu|}{8\pi} \, , \qquad (9)$$

can no longer be neglected for $|\mu| \ll t$. Note, that the sum Z of the contributions Eqs. (8) and (9), is independent of μ and hence of the carrier density [34, 37].

From these observations we conclude that the f-sum rule or $Z(\mu)$ can serve as a quasi-order parameter for the Lifshitz transition, indicating relativistic behavior for $|\mu|/t < 1$ with $Z \approx$ const., as compared to the non-relativistic Fermi-liquid regime for $|\mu| > t$, where $Z(\mu) \approx Z_+(\mu)$ decreases almost linearly with μ. We verified analytically that the derivative of $Z(\mu)$ with respect to μ diverges logarithmically at the Lifshitz transition, $\mu = t$. This reflects a singular behavior of the carrier density similar to that of χ in Eq. (3), since $Z_+ \propto n_c$ for $|\mu|/t \gtrsim 1$.

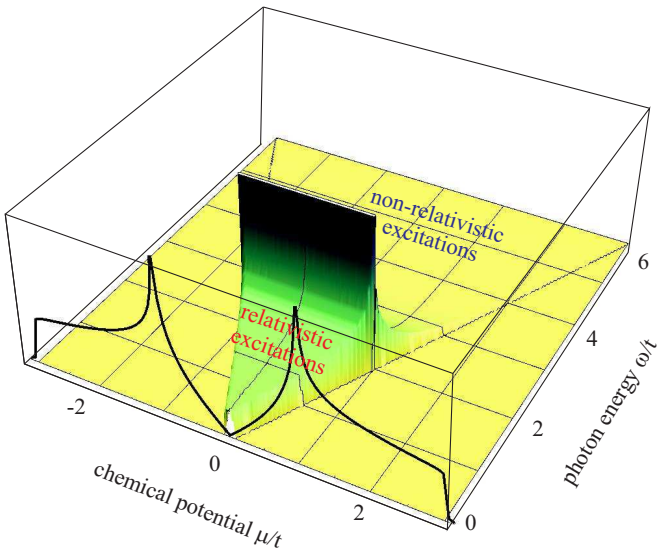

FIG. 4: (Color on line) Spectral distribution $\rho_{\rm ph}(\omega)$ of vertical particle-hole excitations derived from the imaginary part of the polarization function as function of the rescaled chemical potential μ/t and excitation frequency ω/t showing the ESQPT at $\omega/t = 2$ for $|\mu|/t < 1$. Also displayed in the front panel for $\omega = 0$ is the number susceptibilty $\chi = \rho(\mu)/A$ to indicate the corresponding ground-state Lifshitz transitions at $\mu = \pm t$.

We obtained the full spectral distribution $\rho_{\rm ph}(\omega)$ of particle-hole excitations Eq. (5) from explicit analytical expressions for the polarization function. The result for $\Pi_+^R(\omega, \vec{p}; \mu)$ from intraband transitions was first derived in [33]. Here we are particularly interested in the imaginary part of $\Pi_-^R(\omega, \vec{p}; \mu)$ for the interband transitions which reflects the ESQPT in the Dirac-cone region for $|\mu| < t$. For small momenta we computed the spectral density as described in Ref. [36]. The result is summarized in Fig. 4 where we display $\rho_{\rm ph}(\omega)$. In the front panel we have included the number susceptibility $\chi(\mu) = \rho(\mu)/A$, to indicate the two ground-state Lifshitz transitions at $\mu = \pm t$. As in the Dirac cone approximation, interband contributions to $\rho_{\rm ph}(\omega)$ vanish when $\omega < 2\mu$ because the vertical particle-hole excitations are then Pauli blocked. The ESQPT in the particle-hole excitation spectrum at zero momentum transfer is clearly visible in Fig. 4 at $\omega = 2\mu$. There the spectral distribution exhibits a logarithmic divergence which is directly linked

to that of the single-particle DOS at the van Hove singularity Eq. (2). Below this, for $\omega < 2t$ and $\mu < t$, we have the relativistic behavior of the low-frequency excitations as discussed above. Above the ESQPT, for $\omega > 2t$, the density of particle-hole excitations decreases fast with increasing frequency, as it does in the normal Fermi-liquid regime.

Conclusions.– We determined the DOS in high-precision experiments with two superconducting Dirac billiards and recovered the finite-size scaling governing such transitions experimentally and also numerically with Dirac billiards of different sizes and geometries. The DOS we obtain is similar to that of transverse vibrations of an hexagonal lattice and, most importantly, to that of the electronic band structure of finite graphene sheets. In the second part of the letter, we show that the properties of the observed DOS can be described in terms of a QPT and ESQPT arising from the topological Lifshitz neck-disrupting phase transition. We plan now to investigate the features of the oscillations observed in the experimental DOS in Fig. 1. These obviously differ in the frequency range between the van Hove singularities, where the wave propagation is governed by the relativistic Dirac equation, and that, where the non-relativistic Schrödinger equation applies (see Fig. 1). The differences in the amplitudes and the frequencies of the oscillations will be extracted from their Fourier transforms.

This work has been supported by the DFG within the SFB 634. One of us (F.I.) acknowledges support from U.S.D.O.E. Grant DE-FG02-91ER40608.

[1] G. W. Semenoff, Phys. Rev. Lett. **53**, 2449 (1984).
[2] S. Reich, J. Maultzsch, C. Thomsen, and P. Ordejón, Phys. Rev. B **66**, 035412 (2002).
[3] Note, that the electronic energies of graphene take over the rôle of the frequencies in the microwave Dirac billiards.
[4] A. H. Castro Neto, F. Guinea, N. M. R. Peres, K. S. Novoselov, and A. K. Geim, Rev. Mod. Phys. **81**, 109 (2009).
[5] L. Van Hove, Phys. Rev. **89**, 1189 (1953).
[6] Y.-W. Son, S.-M. Choi, Y. P. Hong, S. Woo, and S.-H. Jhi, Phys. Rev. B **84**, 155410 (2011).
[7] M. Bellec, U. Kuhl, G. Montambaux, and F. Mortessagne, Phys. Rev. Lett. **110**, 033902 (2013).
[8] A. Varlamov, V. Egorov, and A. Pantsulaya, Advances in Physics **38**, 469 (1989).
[9] I. Lifshitz, Sov. Phys. JETP **11**, 1130 (1960).
[10] F. Iachello and S. Oss, The Journal of Chemical Physics **104**, 6956 (1996).
[11] W. D. Heiss, F. G. Scholtz, and H. B. Geyer, Journal of Physics A **38**, 1843 (2005).
[12] F. Leyvraz and W. D. Heiss, Phys. Rev. Lett. **95**, 050402 (2005).
[13] P. Cejnar, M. Macek, S. Heinze, J. Jolie, and J. Dobeš, J. Phys. A **39**, L515 (2006).
[14] D. Larese and F. Iachello, J. Mol. Struct. **1006**, 611 (2011).
[15] A. Caprio, M., P. Cejnar, and F. Iachello, Ann. Phys. **323**, 1106 (2008).
[16] A. Richter, in *Emerging Applications of Number Theory,* The IMA Volumes in Mathematics and its Applications, edited by D. A. Hejhal, J. Friedmann, M. C. Gutzwiller, and A. M. Odlyzko (Springer, New York, 1999), vol. 109, p. 479.
[17] H.-J. Stöckmann, *Quantum Chaos: An Introduction* (Cambridge University Press, Cambridge, 2000).
[18] E. Yablonovitch and T. J. Gmitter, Phys. Rev. Lett. **63**, 1950 (1989).
[19] S. Joannopoulos, J. D. Johnson, R. Meade, and J. Winn, *Photonic Crystals. Molding the Flow of Light* (Princeton University Press, Princeton and Oxford, 2008), 2nd ed.
[20] E. I. Smirnova, C. Chen, M. Shapiro, J. Sirigiri, and R. Temkin, Journal of Applied Physics **91**, 960 (2002).
[21] S. Bittner, B. Dietz, M. Miski-Oglu, P. Oria Iriarte, A. Richter, and F. Schäfer, Phys. Rev. B **82**, 014301 (2010).
[22] S. Raghu and F. D. M. Haldane, Phys. Rev. A **78**, 033834 (2008).
[23] P. R. Wallace, Phys. Rev. **71**, 622 (1947).
[24] X. Zhang and Z. Liu, Phys. Rev. Lett. **101**, 264303 (2008).
[25] S. R. Zandbergen and M. J. A. de Dood, Phys. Rev. Lett. **104**, 043903 (2010).
[26] S. Bittner, B. Dietz, M. Miski-Oglu, and A. Richter, Phys. Rev. B **85**, 064301 (2012).
[27] Y. Poo, R.-X. Wu, Z. Lin, Y. Yang, and C. T. Chan, Phys. Rev. Lett. **106**, 093903 (2011).
[28] U. Kuhl, S. Barkhofen, T. Tudorovskiy, H.-J. Stöckmann, T. Hossain, L. de Forges de Parny, and F. Mortessagne, Phys. Rev. B **82**, 094308 (2010).
[29] J. P. Hobson and W. A. Nierenberg, Phys. Rev. **89**, 662 (1953).
[30] J. Lindhard, Det Kgl Danske Vid. Selskab, Matematisk-fysiske Meddelelser **28** (1954).
[31] S. Barkhofen, M. Bellec, U. Kuhl, and F. Mortessagne, Phys. Rev. B **87**, 035101 (2013).
[32] We neglect the physical spin of the electrons which would amount to a doubling of the degrees of freedom.
[33] T. Stauber, Phys. Rev. B **82**, 201404 (2010).
[34] V. N. Kotov, B. Uchoa, V. M. Pereira, F. Guinea, and A. H. Castro Neto, Rev. Mod. Phys. **84**, 1067 (2012).
[35] Y. Blanter, M. Kaganov, A. Pantsulaya, and A. Varlamov, Physics Reports **245**, 159 (1994), ISSN 0370-1573.
[36] B. Dietz *et al.*, to be published.
[37] J. Sabio, J. Nilsson, and A. H. Castro Neto, Phys. Rev. B **78**, 075410 (2008).
[38] P. Noziéres, *Theory of Interacting Fermi Systems*, Advanced Book Classics (Westview Press, 1997).